Non Destructive Testing of Cylindrical Ropes through the Parametric Transformer

Daniele Romano, Tommaso Scozzafava, and Giulio Antonini

UAq EMC Laboratory, Department of Industrial and Information Engineering and Economics
University of Study of L'Aquila, 67100 L'Aquila, Italy
giulio.antonini@univaq.it

Abstract – In order to ensure the safe operation of wire ropes, non-destructive testing methods are being applied to inspect wire ropes. Any geometrical discontinuity in magnetic permeability in the magnetized wire rope will impact the magnetic field conveyed by the rope, under a proper excitation. In this work, the electromagnetic device known as "parametric transformer" has is proposed for the non-destructive testing of ferromagnetic bodies having cylindrical symmetry, as tubes and ropes. The principle of its functioning is described by means of an equivalent magnetic network and a more rigorous approach using the Partial Element Equivalent Circuit (PEEC) method. Then, the proposed principle has been tested experimentally through the realization of a model which has confirmed the expected results.

Index Terms – Cylindrical ropes, non-destructive testing, parametric transformer.

I. INTRODUCTION

Steel wire ropes are the basic and important elements of loading, and, as such, they are widely employed in many fields, such as mining, architecture, transport, etc. Safe use of the wire ropes depends on their condition. Deterioration of a wire rope leads to a reduction of the wire rope safety factor. The manual inspection such as visual observing is often used to check wire ropes but it can only detect surface flaw, so this method is not that reliable. On the other hand, destructive inspection can only bring the information about tested part of rope and requires spare lengths of the rope be available for such test. Hence, non-destructive testing (NDT) for steel wire ropes has received increasing interest. The most popular NDT inspection methods include acoustic emission, electromagnetic methods [1, 2, 3], imaging methods. Among the electromagnetic methods, the most common technique applied in the NDT of ferromagnetic ropes are based on the magnetic inspection (MI) and in particular on the magnetic flux leakage (MFL) [4] making use of testing sensor, signal conditioning unit and computer system unit.

In this work a different approach is proposed. In particular, the parametric transformer is used to detect imperfections occurring in cylindrical ropes. Indeed, the principle is rather simple. Even small defects in the rope cause a magnetic flux to appear in the central limb of the transformer which is usually inactive in absence of defects. This flux causes an induced voltage on a sensing coil located on the same limb which can be easily measured by a voltage meter. The proposed method can be adopted in case of quite long ropes as those used in the elevators, cableways or skilifts when the length of the rope is in the range of tens, hundreds or even thousands of meters, to continuously monitor the state of the rope.

The paper is organized as follows. Section II briefly describes the parametric transformer (PT) and explains how it can be used for NDT purposes. The ideal model of the PT is presented in Section III and a simplified solution is proposed. In order to more accurately model the PT and give evidence to its capability to be used fo NDT purposes, the Partial Element Equivalent Circuit method is used. It is summarized in Section IV. The numerical results are presented in Section V confirming also numerically that the PT is effective in detecting small defects occurring in cylindrical ropes. The conclusions are drawn in Section VII.

II. THE PARAMETRIC TRANSFORMER

The parametric transformer (PT thereafter) is a "two ports" device based on any special symmetric magnetic circuits which couples an input coil with an output coil; this coupling is inactive until the above mentioned symmetry is guaranteed, and the mutual induction coefficient is zero. There are many types of PT with different shape of the magnetic circuit [5]; we chose the particular one shown in Fig. 1, in which

Submitted On: July 27, 2018
Accepted On: May 7, 2019

the magnetic circuit is completed by a sample of the material to be tested, so that any defect present in the sample breaks the magnetic symmetry, the mutual induction coefficient turns into a non-zero value and an output signal is obtained if the input port is powered.

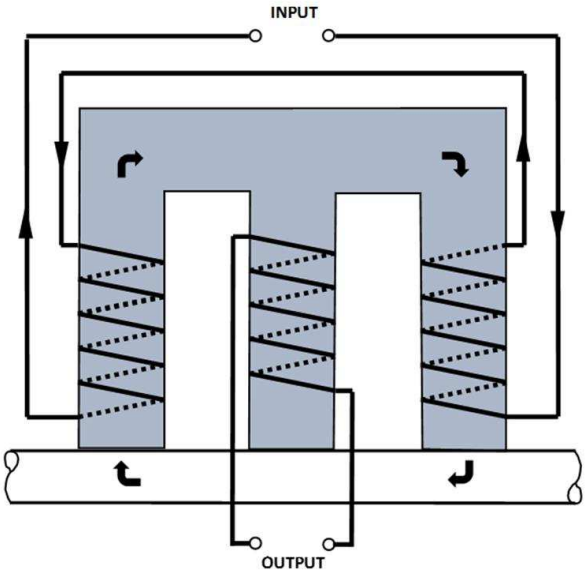

Fig. 1. Parametric transformer.

In Fig. 1, the coordinate directions of the currents and the magnetic fluxes are highlighted in order to clarify the functioning principle.

The equivalent magnetic network of this device is composed by:

- the left and right outer branches, including also their horizontal part, both of the same reluctance $\mathcal{R}$;
- the central branch of reluctance $\mathcal{R}_\mathcal{C}$;
- the sample of the material ferromagnetic to be tested, a part of which completes the magnetic mesh composed by the above mentioned outward branches; we set $\mathcal{R}_\mathcal{S} + \mathcal{R}_\mathcal{S} = 2\mathcal{R}_\mathcal{S}$ reluctance of this part if the sample is integer, but we set $2\mathcal{R}_\mathcal{S}+\mathcal{R}_\mathcal{D}$ if a defect of additional reluctance $\mathcal{R}_\mathcal{D}$ is present in its left or right part;
- two equal coils winding the two outward branches, powered by the same current, provides two equal exciting m.m.f. $\mathcal{F}$, having the same directions along the external magnetic mesh composed by the two outer branches and the portion of body under testing;
- a coil winding the central branch, providing an output signal if a variable magnetic flux ϕ appears in it.

In the first rough approach of the analysis of this device we assume:

- the magnetic fluxes are restricted inside the PT and inside the sample, namely no leakage flux exists;
- the behaviour of the PT and of the sample is linear.

III. IDEAL MODEL

If the aforesaid hypotheses are satisfied, we may draw the magnetic equivalent network of the Fig. 2. We assume the coils are powered by a steady state current; if the body to be tested may slide along (and in contact with) the three branches, a flux ϕ appears in the central branch when a defect of the sample is present; in Fig. 2 we suppose the existence of a defect in the right side.

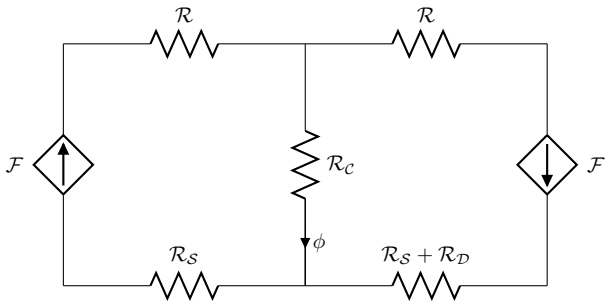

Fig. 2. Equivalent magnetic network.

If the sliding sample does not have any defect (that is if $\mathcal{R}_\mathcal{D} = 0$) a magnetic flux, whose value obviously equals $2\mathcal{F}/(2\mathcal{R}+2\mathcal{R}_\mathcal{S})$, is present only in the outer branches of the PT; consequently $\phi = 0$ and no output signal is present. If a defect occurs, the analysis (plain but cumbersome) of this network provides for the above flux the value:

$$\phi = \mathcal{F}\mathcal{R}_\mathcal{D}/[(\mathcal{R}+\mathcal{R}_\mathcal{C}+\mathcal{R}_\mathcal{S})(\mathcal{R}+\mathcal{R}_\mathcal{C}+\mathcal{R}_\mathcal{S}+\mathcal{R}_\mathcal{D})-\mathcal{R}_\mathcal{C}]. \quad (1)$$

Obviously the amplitude of the electrical output signal depends on the derivative of the flux ϕ and therefore on the flow rate of the sample, which may not be sufficient to obtain an adequate level; if, however, the feeding occurs in a sinusoidal regime, this limitation disappears and in addition there is the advantage of being able to perform the test even when stationary.

IV. BASIC PEEC FORMULATION

In order to verify the feasibility of the proposed methodology to detect defects in cylindrical ropes, the Partial Element Equivalent Circuit (PEEC) method [6] is used to model the parametric transformer and the rope. The PEEC method is based

on the volume equivalence principle of Maxwell's equations and use the electric field integral equation (EFIE) and the continuity equation. When conductors, dielectrics and magnetic materials are considered, the natural physical quantities which are usually adopted to express the magnetic vector potential are the electrical and polarization current densities and magnetization. Furthermore, the scalar electric potential is also used. Typically, rectangular basis functions are used to expand these quantities and to test the EFIE and continuity equation, based on the Galerkin's testing procedure. It results in the following set of equations:

$$\begin{bmatrix} j\omega\mathbf{P}^{-1} & -\mathbf{A}^T & \mathbf{0} \\ \mathbf{A} & \mathbf{Z}_s + j\omega\mathbf{L}_p & j\omega\mathbf{L}_m \\ \mathbf{0} & \mathbf{D} & \mathbf{T} \end{bmatrix} \cdot \begin{bmatrix} \mathbf{\Phi} \\ \mathbf{I} \\ \mathbf{M} \end{bmatrix} = \begin{bmatrix} \mathbf{I}_s \\ \mathbf{0} \\ \mathbf{GI}_s \end{bmatrix}, \tag{2}$$

where $\mathbf{P}$ accounts for the coefficients of potential, $\mathbf{L}_p$ is the partial inductance matrix, $\mathbf{L}_m$ represents the induced effects due to time varying magnetization, $\mathbf{D}$ and $\mathbf{T}$ matrices describe the constitutive relation of the magnetic field and $\mathbf{A}$ is the connectivity matrix. Matrix $\mathbf{Z}_s$ is diagonal with the self impedances of elementary volumes, which reduce to resistances for conductors [7] and the impedances of the excess capacitance [8] for dielectrics. Finally, $\mathbf{I}_s$ represents the independent current source which is assumed to drive the excitation coils. The term $\mathbf{GI}_s$ represents the magnetic flux density produced by the forced current. The derivation of (2) and the analytical formulas to fill matrices in (2) are detailed in [9, 10]. The time domain counterpart is straightforward to be obtained.

V. NUMERICAL TESTS

A 3D PEEC model of the parametric transformer has been set. It is shown in Fig. 3. The conductivity of the magnetic core is $\sigma = 10^6$ S/m and its relative magnetic permeability is $\mu_r = 400$ while the coils are made of copper ($\sigma = 5.8 \cdot 10^7$ S/m).

In addition a rope with a small defect (a hole with volume 1 cm^3) has been placed in the air-gap as shown in Fig. 3. The conductivity of the rope is $\sigma = 10^4$ S/m and its relative magnetic permeability is $\mu_r = 300$.

The geometrical parameters for the $x-y$ plane are given in Fig. 4. Respect to the z axis, both the rope and the magnetic core are 20 mm thick. The coils are 10 mm thick in all directions and the spacing between these and the magnetic core is 1 mm. Finally, the spacing between the rope and the magnetic core is 0.5 mm.

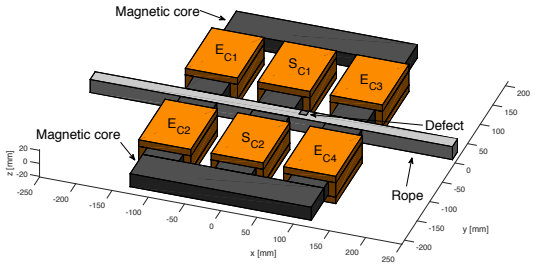

Fig. 3. 3D view of the PEEC model of the parametric transformer.

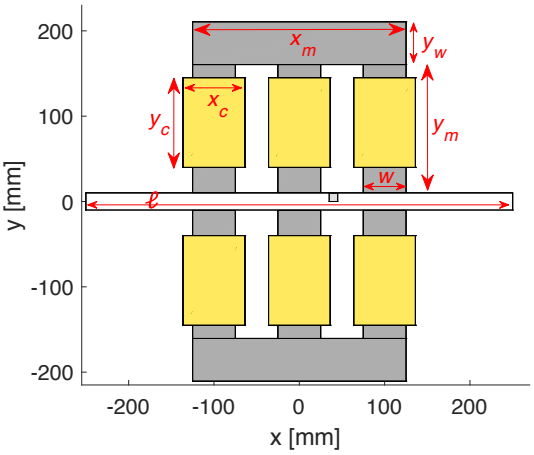

Fig. 4. Configuration of the parametric transformer, $x_m = 250$, $y_w = 50$, $y_m = 150$, $w = 50$, $x_c = 72$, $y_c = 105$ and $\ell = 500$ (all dimensions are in mm).

The excitation coils, namely $\mathrm{E_{C_1}}$, $\mathrm{E_{C_2}}$, $\mathrm{E_{C_3}}$ and $\mathrm{E_{C_4}}$, are driven by a 10 A sinusoidal current source (2.5 A for coil) varying at 50 Hz.

The analysis has been performed by using an uniform mesh resulting in by 9297 surface nodes, 29554 inductive branches and 3034 magnetic cells in the case of the absence of the defect for the rope while in the presence of the defect the mesh is constituted by 9297 nodes, 30304 inductive branches and 3180 magnetic cells.

The voltage revealed by the sensor coil $\mathrm{S_{C_1}}$ is reported in Figs. 5 and 6 for both the cases of absence and presence of the defect, respectively. As it is clearly seen, even a small defect, causes significant differences in the sensed voltage.

Finally, Figs. 7 and 8 show the z component ($|B_z|$) of the magnetic field for both the cases of absence and presence of the defect, respectively, at the time instant in which the excitation current is maximum (the surface in the x-y plane is located in the middle of the structure respect to the z axis). As before, a small defect causes significant differences also in the magnetic field.

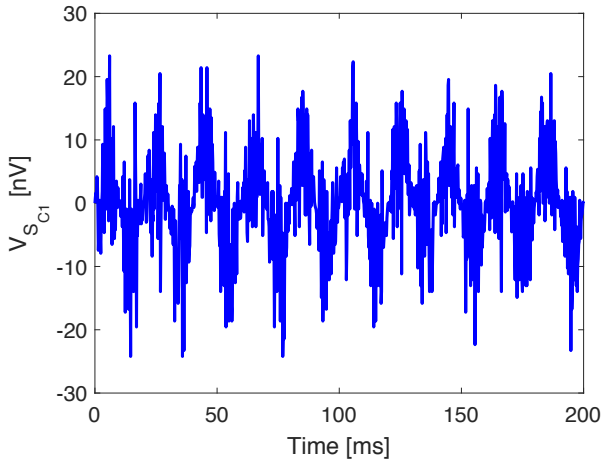

Fig. 5. S_{C_1} voltage without defect.

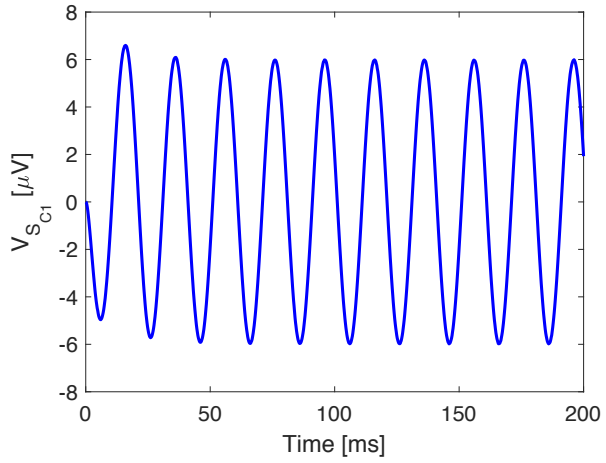

Fig. 6. S_{C_1} voltage in the presence of the defect.

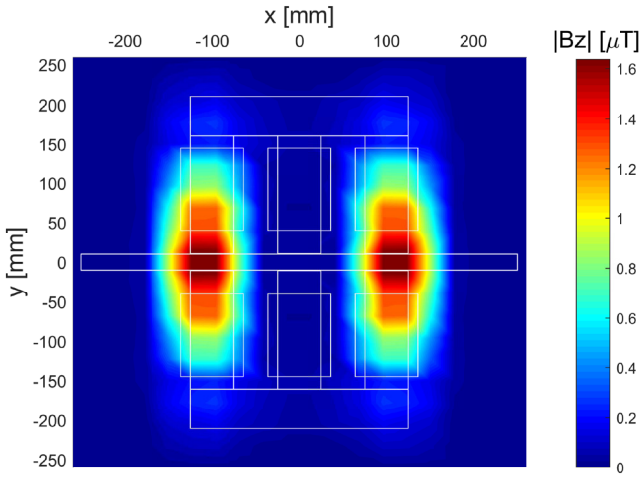

Fig. 7. $|B_z|$ without defect.

VI. EXPERIMENTAL SET-UP

Having described the operating principle, we describe now how we have realized the experimental

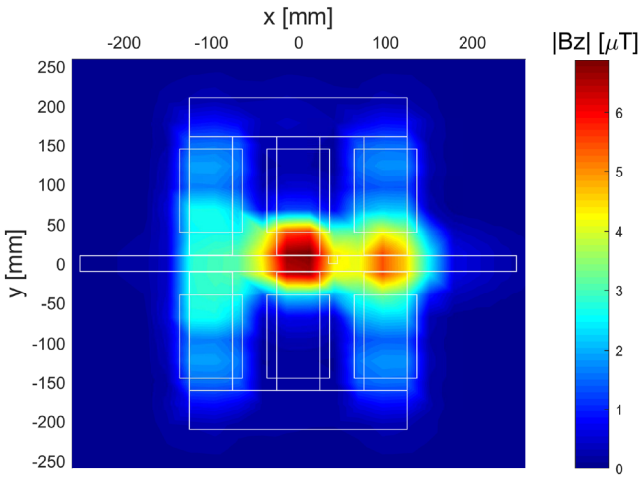

Fig. 8. $|B_z|$ in the presence of the defect.

fixture. We used for it the magnetic laminations of a common three-phase transformer; for a former prototype of this device it was chosen the arrangement shown in Fig. 1 [11]. In order to better identify the defects of the sample, the initial prototype has been developed as described in Fig. 1. Hence, it is constituted by two PTs mounted in opposite position; their outputs are connected in series, in order to obtain the sum of the two signals, with a significant improvement of the sensitivity.

The scheme of Fig. 2, which was used to clarify the operating principle, can no longer be used for quantitative evaluations, either because in the sinusoidal regime equation (1) should be recalculated in the complex field, and because it does not take into account the inevitable leakage flux that does not remain confined into the magnetic material under analysis. The estimation of this leakage flux is not easy. The rope sample has been modeled with a geometry composed of elementary parallelepipeds, in one of which an interruption has been introduced that simulates the defect. The permeability and resistivity values of the magnetic circuit are the normal values for a sheet from transformers, while for the cable we assumed the estimate of 400 as the average "iron-air" value of the relative permeability.

To evaluate the efficiency of the device, we carried out several series of measurements on a sample of parametric transformer, shown in Fig. 9. In the beginning, a piece of rope free of defects has been used. Since the operation must also take place with the rope in motion and this involves the existence of an air gap whose influence cannot be neglected, we have simulated its existence in the measurements (which were of the static type) by inserting two strips in cardboard 0.5 mm thick between the

Fig. 9. Experimental set-up.

sample and the surfaces of the pole pieces of the device. We fed the input with a 50 Hz sinusoidal generator at variable voltage, of which we measured the effective current and voltage values; of the signal at the output we measured the effective value in voltage. With the aforementioned sample, we have carried out a series of preliminary measurements that have served to highlight the inevitable constructional asymmetry of the apparatus, which produce a "bias" signal which must be taken into account in the results. Then the measurements were performed in the presence of defects that we simulated using the same integral sample to which we added a small piece of elementary wire at one of the two spaces between the poles.

Since the measurement is of the differential type, the equivalent of a lack of the same wire volume is obtained at the other space between the two poles. The results of the measurements were collected in Table 1, made up of 7 columns; in the first and in the second ones respectively, the effective values of the current C_{in} (in A) and of the voltage V_{in} (in V) at the input are indicated, having chosen to impose current values at constant intervals of 0.10 A; in the third column we have indicated the output voltage of "bias" (V_{bias}) detected with the rope sample intact; in the fourth and fifth columns we have indicated,

Table 1: Experimental results

C_{in}	V_{in}	V_{bias}	V_{outR}	V_{outL}	S_R	S_L
0.10	3.0	0.012	0.019	0.013	1.58	1.08
0.20	4.0	0.013	0.027	0.020	2.08	1.54
0.30	6.0	0.013	0.037	0.029	2.85	2.23
0.40	8.0	0.015	0.060	0.036	4.00	2.40
0.50	10.0	0.016	0.065	0.042	4.06	2.63
0.60	13.0	0.018	0.060	0.049	3.33	2.72
0.70	15.0	0.018	0.067	0.060	3.72	3.33
0.80	17.0	0.018	0.077	0.070	4.28	3.89
0.90	20.0	0.026	0.104	0.083	4.00	3.19
1.00	22.0	0.027	0.110	0.085	4.07	3.15
1.10	24.0	0.027	0.103	0.093	3.81	3.44
1.20	26.0	0.028	0.109	0.095	3.89	3.39
1.30	28.0	0.028	0.106	0.096	3.79	3.43
1.40	30.0	0.029	0.123	0.083	4.24	2.86
1.50	33.0	0.029	0.122	0.085	4.21	2.93
1.60	34.0	0.029	0.124	0.085	4.28	2.93
1.70	37.0	0.030	0.134	0.085	4.47	2.83
1.80	39.0	0.030	0.126	0.095	4.20	3.17
1.90	39.0	0.031	0.140	0.095	4.52	3.06
2.00	42.0	0.032	0.144	0.101	4.50	3.16
2.10	45.0	0.033	0.146	0.095	4.42	2.88
2.20	46.0	0.034	0.135	0.101	3.97	2.97
2.30	48.0	0.036	0.140	0.101	3.89	2.81
2.40	50.0	0.037	0.145	0.114	3.92	3.08
2.50	52.0	0.039	0.167	0.114	4.28	2.92

respectively, the output voltage with the fault positioned first on the right (as in Fig. 2) and then on the left of the central pole (V_{outR} and V_{outL}); in the sixth and seventh columns we have reported the respective useful signals (S_R and S_L) calculated as the ratio between the two aforementioned voltages and that of "bias"; S_R and S_L are obviously adimensional quantities. Figure 10 shows the measured voltages in presence of the defect at right (V_{outR}) and left (V_{outL}) of the central pole along with the bias voltage (V_{bias}).

A. Discussion

It can be seen how, while the input current increases with a constant pitch, the corresponding voltage does not increase with the same regularity; this is due to the fact that the rope, being composed of strands wound in a spiral, configures with the surfaces of the poles an average air gap that is variable and depends on the position assumed from time to time, when the defect is transferred from one part to the other of the sample. In other words, the reluctances $\mathcal{R}$ and $\mathcal{R}_{\mathcal{C}}$ of the scheme in Fig. 2 comprise the air gaps and are affected by their variability. It can also be noted that the state of the magnetic materials of the laminations and of the cable is always in the linearity zone, since the module of the

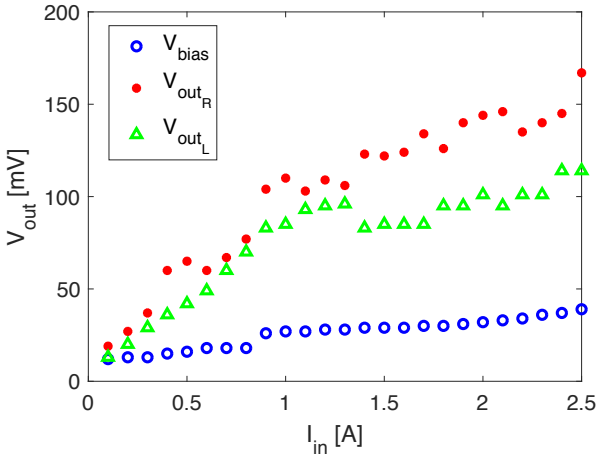

Fig. 10. Measured voltages in presence of the defect at right (V_{outR}) and left (V_{outL}) of the central pole and bias voltage (V_{bias}).

input impedance V_{in}/C_{in} has a very little variation between the minimum and maximum values of 20.0 Ω and 22.2 Ω (as is easy to verify) throughout the excitation current range between 0.10 A and 2.50 A. Its small variability is due to the not exact reproducibility of the air gaps during all the measurements. The magnitude of the fault signals (even these vary in an uncoordinated way, again due to the variability of the air gaps between one measurement and the other) seems sufficient to achieve the purpose for which the apparatus was designed, especially considering how the artificial failure has been achieved.

VII. CONCLUSIONS

The parametric transformer has been found effective in the detection of the defects present in a rope. A simple derivation has been presented along with a numerical simulation have given evidence to the theoretical claim. Furthermore, an experimental setup has been built and has confirmed the theoretical results, in spite of the complicated shape of the rope section which caused, owing to the variability of the air gap, little anomalies in the measurements. No doubt these anomalies disappear, if the material was a sample of a simple tube. In order to improve the output signal for the ropes, it is required a reduction of the air gap reluctances, achievable by an enlargement of the three poles along the axis of the sample. Despite these limitations, a satisfactory sensitivity has been achieved, confirming the possibility to use the parametric transformer as an effective device for non destructive testing of cylindrical ropes.

Acknowledgments

The authors acknowledge ELITAL s.r.l. of L'Aquila for having built and made available the parametric transformer.

REFERENCES

[1] M. Parise, "An exact series representation for the EM field from a circular loop antenna on a lossy half-space," *IEEE Antennas and Wireless Propagation Letters*, vol. 13, pp. 23–26, 2014.

[2] M. Parise, "On the surface fields of a small circular loop antenna placed on plane stratified earth," *International Journal of Antennas and Propagation*, vol. 2015, pp. 1–8, 2015.

[3] M. Parise, "Full-wave analytical explicit expressions for the surface fields of an electrically large horizontal circular loop antenna placed on a layered ground," *IET Microwaves, Antennas and Propagation*, vol. 11, pp. 929–934, 2017.

[4] C. Tomasz, P. Grzegorz, T. Takashi, and B. Bartosz, "Evaluation of fatigue-loaded steel samples using fusion of electromagnetic methods," *Journal of Magnetism and Magnetic Materials*, vol. 310, pp. 2737–2739, 2007.

[5] E. S. Tez and I. R. Smith, "The Parametric Transformer: A Power Conversion Device Demonstrating the Principles of Parametric Excitation," *IEEE Transactions on Education*, vol. E-27, no. 2, p. 9, 1984.

[6] A. E. Ruehli, G. Antonini, and L. Jiang, *Circuit Oriented Electromagnetic Modeling Using the PEEC Techniques*, Wiley-IEEE Press, 2017.

[7] A. E. Ruehli, "Equivalent circuit models for three dimensional multiconductor systems," *IEEE Transactions on Microwave Theory and Techniques*, vol. MTT-22, no. 3, pp. 216–221, Mar. 1974.

[8] A. E. Ruehli and H. Heeb, "Circuit models for three-dimensional geometries including dielectrics," *IEEE Transactions on Microwave Theory and Techniques*, vol. 40, no. 7, pp. 1507–1516, Jul. 1992.

[9] D. Romano and G. Antonini, "Quasi-Static Partial Element Equivalent Circuit Models of Linear Magnetic Materials," *IEEE Transactions on Magnetics*, vol. 51, no. 7, pp. 1–15, Jul. 2015.

[10] L. Lombardi, D. Romano, and G. Antonini, "Analytical Formula for the Magnetic-to-Electric Field Coupling of Magnetization in the Partial Element Equivalent Circuit Method," *IEEE Transactions on Magnetics*, vol. 54, no. 10, pp. 1–12, Oct. 2018.

[11] T. Scozzafava, "Differential magnetoscope," Italian Ministry of Industry, Italian Patent N.1182775, Oct. 1987.

Daniele Romano was born in Campobasso, Italy, in 1984. He received the Laurea degree in computer science and automation engineering in 2012 from the University of L'Aquila, L'Aquila, Italy. He received the Ph.D. degree in 2018. Since 2012 he has been with the UAq EMC Laboratory, University of L'Aquila, focusing on EMC modeling and analysis, algorithm engineering and speed-up techniques applied to EMC problems.

Tommaso Scozzafava received the Laurea degree (*cum laude*) in industrial electrical engineering from the University of Rome "La Sapienza", Italy, in 1960. Since 1971, he has been with the University of L'Aquila, where he has been an Associate Professor from 1982 until 2002. His scientific interests are in the field of electrical engineering and measurements.

Giulio Antonini received the Laurea degree (*cum laude*) in electrical engineering from the University of L'Aquila, L'Aquila, Italy, in 1994 and the Ph.D. degree in electrical engineering from University of Rome "La Sapienza" in 1998. Since 1998, he has been with the UAq EMC Laboratory, University of L'Aquila, where he is currently a Professor. He has coauthored the book "*Circuit Oriented Electromagnetic Modeling Using the PEEC Techniques*", (Wiley-IEEE Press, 2017). His scientific interests are in the field of computational electromagnetics.